ChemComm

Accepted Manuscript

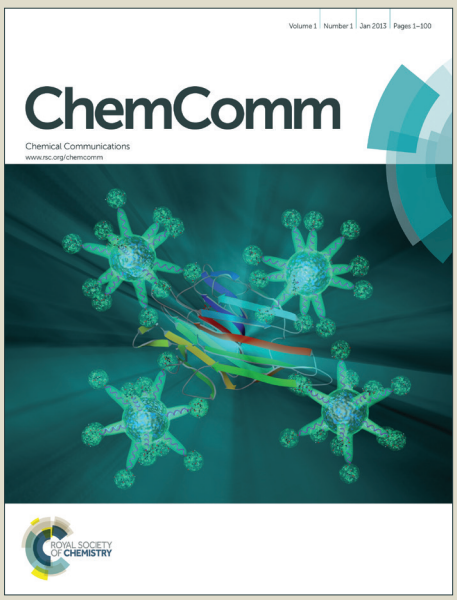

ROYAL SOCIETY OF CHEMISTRY

www.rsc.org/chemcomm

Journal Name

COMMUNICATION

Mesoporous Materials Modified by Aptamers and Hydrophobic Groups Assist Ultra-sensitive Insulin Detection in Serum

Received 00th January 20xx,
Accepted 00th January 20xx

DOI: 10.1039/x0xx00000x

www.rsc.org/

Chang Lei,[a] Chun Xu,[a] Owen Noonan,[a] Anand Kumar Meka,[a] Long Zhang,[a] Amanda Nouwens[a,b] and Chengzhong Yu*[a]

ABSTRACT: A novel mesoporous material modified with both insulin-binding-aptamer and hydrophobic methyl groups is synthesized. With rational designed pore structures and surface chemistry, this material is applied in sample pre-treatment for ELISA, enables a quantification (0.25-5 pg ml^{-1}) of insulin in serum, 30-folds enhancement of limit-of-detection comparing to commercial ELISA kit.

Detection of insulin is essential for disease diagnosis,[1] pathological research and doping control.[2, 3] Due to low abundance and complexity in biological samples (e.g. serum),[4] sensitive detection of insulin remains a long-standing challenge. Many strategies such as enzyme linked immunosorbent assay (ELISA), radioimmunoassay (RIA)[3], immunoassay followed by liquid chromatography–tandem mass spectrometry (LC-MS/MS)[5], solid phase extraction (SPE),[6, 7] photolytic-electrochemical detection[8] and high performance liquid chromatography(HPLC) coupled with UV absorbance[9, 10] have been developed for insulin detection. However, for detection in complicated samples containing very low levels of insulin,[3, 11] it is essential to pre-treat and enrich samples to increase the detection sensitivity.[12, 13]

Recently, the application of nanotechnology has led to significant advances in biomolecule enrichment and identification.[14, 15] In particular, mesoporous materials with controllable pore structure and surface chemistry have attracted much attention.[13, 14] Our previous study showed that hydrophobic modification of pore surface with a suitable pore size is beneficial to insulin enrichment.[13] However, the advantages provided by optimised pore size and hydrophobicity do not address the specific binding issue. It is expected that mesoporous materials functionalized with specific binding molecules will minimise non-specific adsorption in serum and selectively enrich low abundance targets.

Antibody is a well-known specific binding molecule with high affinity of antigen-antibody binding. There are several reports on mesoporous silica materials functionalized with antibodies (generally on the external surface) for protein capture. Despite the stability issue,[17] it is difficult to modify antibody inside the mesopores due to the large molecular size (*e.g.* IgG 20 nm).[18] Although large-pore materials are available,[19] previous study has shown that a large pore size is not favoured for the insulin enrichment.[13] Alternatively, aptamers are effective substitutes for antibodies[17] and have advantages such as small molecular size, excellent stability, and low cost.[20] It is reported that the insulin binding aptamer (IBA) with a two-repeat parallel G-quadruplex structure can selectively bind to insulin.[20, 21] A study used IBA modified plate for insulin detection, achieving a limit-of-detection (LOD) in standard solution and serum of 5 and 20 ng ml^{-1}, respectively.[22] IBA was modified onto carbon nanotubes for insulin extraction from pancreatic INS-1 cells with an LOD of 58 ng ml^{-1}.[20] However, there is no report on the modification of mesoporous materials by IBA for insulin detection. Furthermore, although aptamers have been modified onto mesoporous materials for drug delivery,[23] there is no report on co-modification of hydrophobic groups and aptamers for insulin enrichment.

In this study, the conjugation of IBA and methyl groups on mesoporous silica is reported for sensitive insulin detection. Aminopropyl(diethoxy)methylsilane (APDEMS) is used to modify mesoporous silica to introduce two functional groups ($-CH_3$ and $-NH_2$ for further IBA conjugation) simultaneously on one silanol (Scheme 1a), which overcomes the challenges typically encountered in two-step modification processes whereby the first modification step consumes a large number of available silanols and reduces the density of the second functionality.[24] The resultant functional mesoporous silica enables efficient enrichment of insulin in serum (Scheme.1b) prior to ELISA test, achieving a quantification range of 0.25-5 pg ml^{-1} of insulin in serum, 30 folds enhancement compared to commercial ELISA kits alone and more sensitive than other literature reports (Table. S1).[5-7, 9, 10, 20, 22, 25-30]

[a] *Australian Institute for Bioengineering and Nanotechnology, The University of Queensland, Brisbane, QLD 4072, Australia. E-mail: c.yu@uq.edu.au*
[b] *School of Chemistry and Molecular Biosciences, The University of Queensland, Brisbane, QLD 4072, Australia.*
Electronic Supplementary Information (ESI) available: experimental details, characterization data. See DOI: 10.1039/x0xx00000x

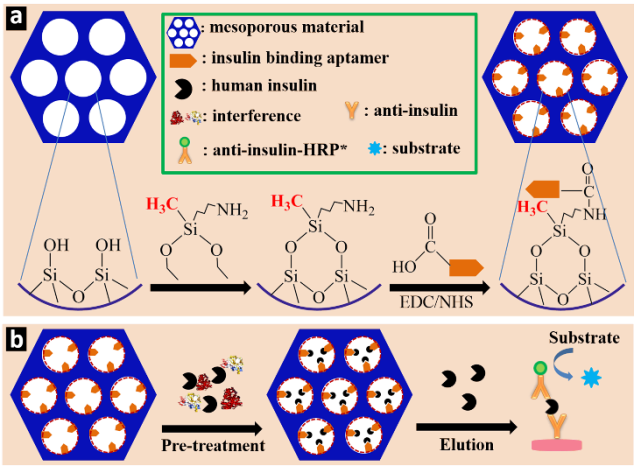

Scheme 1 Schematic illustration showing the (a) synthesis process of insulin binding aptamer and hydrophobic modified mesoporous materials for insulin enrichment; (b) process of pre-treatment coupling ELISA. * HRP: Horseradish peroxidase.

To demonstrate the effect of surface chemistry on insulin enrichment, three functionalized mesoporous silica materials were prepared using SBA-15[31, 32] as the parent material. The first one contained both -CH_3 and -NH_2 groups (named as SBA-15-CH_3-NH_2). The second material was prepared with -NH_2 but without -CH_3 group (SBA-15-NH_2) in order to compare the effect of hydrophobic modification. The third one was prepared with both -CH_3 and -NH_2 groups on the outer surface [SBA-15-CH_3-NH_2 (out)] in order to confirm the surface modification inside the mesopores. After linking IBA to -NH_2, the corresponding materials are named as SBA-15-CH_3-IBA, SBA-15-IBA and SBA-15-CH_3-IBA (out).

The small-angle X-ray scattering (SAXS) patterns of SBA-15 (Fig. S1a), SBA-15-NH_2 (Fig. S1b), SBA-15-CH_3-NH_2 (Fig. S1c) and SBA-15-CH_3-NH_2 (out) (Fig. S1d) are shown in Fig. S1. In each pattern, three well-resolved diffractions can be indexed to the 100, 110, and 200 reflections of an ordered two-dimensional hexagonal mesostructure. For SBA-15, SBA-15-CH_3-NH_2 and SBA-15-NH_2, the diffractions appear at the same position corresponding to a cell parameter (*a*) of 11.3 nm, suggesting that the nanostructure is well maintained after modification. For SBA-15-CH_3-NH_2 (out), the 100 diffraction shifts to the small angle range with an increased *a* of 11.9 nm. Moreover, the 200 diffraction has an obviously higher intensity compared to 110 peak (Fig. S1d). The above observation is attributed to the difference in sample preparation. Compared to the first three samples based on calcined SBA-15, SBA-15-CH_3-NH_2 (out) was prepared starting from as-synthesized SBA-15 followed by modification and surfactant extraction. The silica matrix shrinkage is less during the extraction process, leading to a slightly larger unit size. The change in relative intensity between 110 and 200 diffractions can be attributed to the the thickness of silica walls as reported previously.[33]

Transmission electron microscopy (TEM) images in Fig. S2 display the ordered pore channels of SBA-15 (Fig. S2a) with different modifications, including SBA-15-CH_3-NH_2 (Fig. S2b), SBA-15-NH_2 (Fig. S2c) and SBA-15-CH_3-NH_2 (out) (Fig. S2d). Nitrogen adsorption isotherms for all silica materials are typical type IV with capillary condensation of nitrogen occurring at a relative pressure (P/P0) in the range of 0.60 and 0.80. The Barrett–Joyner–Halenda (BJH) model was used to calculate the pore size distribution curves from the adsorption branch (Fig. S3, Table 1). The pore sizes of SBA-15, SBA-15-CH_3-NH_2, SBA-15-NH_2 and SBA-15-CH_3-NH_2 (out) were measured to be 8.0, 6.68, 6.70, and 7.1 nm (Table 1), respectively. Decreases in pore size are observed for modified materials when compared to pristine SBA-15 (pore size 8.0 nm) due to the occupation of the pore by modified groups. The fourth material (SBA-15-CH_3-NH_2 (out)) also showed a decrease in pore size compared to the pristine SBA-15 (8.0 to 7.1 nm), but not as much as SBA-15-CH_3-NH_2 (6.68 nm) and SBA-15-NH_2 (6.70 nm), consistent with SAXS results. The surface area and pore volume of all the materials are listed in Table 1.

FTIR spectroscopy was used to confirm modifications (Fig. S4), revealing two peaks at around 2900 cm^{-1} which indicate the successful incorporation of -CH_3 groups (Fig. S4). ζ potential measurements show that the pristine SBA-15 (Table. 1) is negatively charged due to deprotonation of the -OH group. For all the modified materials, the positive ζ potentials suggest the successful modification with -NH_2 group.

For the conjugation of IBA and nanomaterials, we followed the well-developed method which used N-(3-Dimethylaminopropyl)-N'-ethylcarbodiimide hydrochloride (EDC) as a reagent.[35, 36] In order to characterize materials after IBA functionalization, TEM images for SBA-15-CH_3-IBA were recorded (Fig. 1), which show ordered pore channels from the 100 (Fig. 1b) and 110 (Fig. 1b) directions, confirming that the originally ordered SBA-15 pore structure remains after aptamer modification. We did not conduct the nitrogen adsorption test (each test usually requires a minimum of 5 mg sample) for IBA modified materials due to the relative high price of IBA (even it is cheaper than antibodies).

Table 1. Pore size, surface area, pore volume and zeta potential of materials

Sample	Pore size (nm)	SBETa (m2/g)	Vpb (cm3/g)	ζ potential
SBA-15	8.00	578	0.98	-17.5
SBA-15-CH3-NH2	6.68	297	0.53	35.6
SBA-15-NH2	6.70	286	0.46	36.7
SBA-15-CH3-NH2(out)	7.10	302	0.51	30.6

[a]BET surface area. [b]Total pore volume.

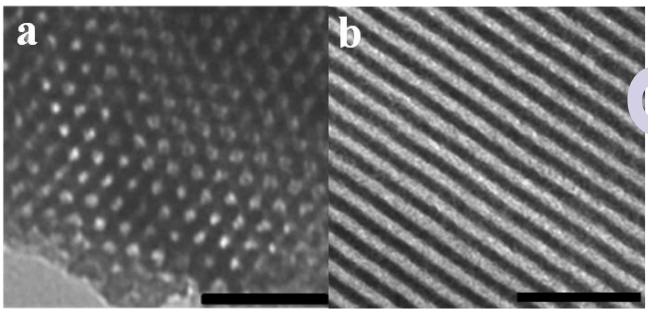

Fig. 1 TEM images of SBA-15-CH_3-IBA viewed (a) parallel and (b) perpendicular to the channel direction of SBA-15. Scale bar: 50 nm.

The surface modification of various groups was also confirmed by X-ray photoelectron spectroscopy (XPS) analysis. Compared to unmodified SBA-15 (Fig. 2a), the existence of nitrogen and an increased amount of carbon in the case of SBA-15-CH_3-NH_2 (Fig. 2b) suggest the successful functionalization of both -CH_3 and -NH_2. XPS survey was also conducted to investigate the modification of IBA. The carbon spectrum of SBA-15-CH_3-NH_2 (Fig. 2c) can be well-fitted to two peaks at 284.8 and 286.1 eV, which are attributed to the binding energies of carbon atoms bonded to C/Si and N, respectively. For SBA-15-CH_3-IBA (Fig. 2d), the spectrum reveals four peaks at 284.8, 285.7, 286.8 and 288.6 eV, which correspond to the binding energies of C-C/C-Si, C-N, C=O and N-C=O respectively. The existence of C=O suggest the successfully modification of IBA.

To find out the optimised material for insulin enrichment, the enrichment efficiency of all groups were compared. The biological system selected for testing was horse serum. In order to remove interferences arising from non-target components in the complex bio-sample, a prior purification step using MOSF-CH_3 was applied using a literature protocol to remove large proteins before the enrichment step.[13] Fig. S5a displays the MS spectrum obtained from the untreated insulin solution (10 ng ml^{-1}). No signal can be detected due to the low insulin concentration. When applying the designed SBA-15-CH_3-IBA for insulin enrichment in a low concentration of 0.05 ng ml^{-1}, both single and double charged peaks are observable (Fig. S5b). For the pre-treatment with SBA-15-IBA and SBA-15-CH_3-IBA (out), the detection limits are 1 ng ml^{-1} (Fig. S5c) and 0.5 ng ml^{-1} (Fig. S5d), respectively. The results show that the SBA-15-CH_3-IBA material (Fig. S5b) has the highest detection sensitivity among all the groups due to the specific binding from IBA, hydrophobic interaction from -CH_3 and size selective effect from mesopores.

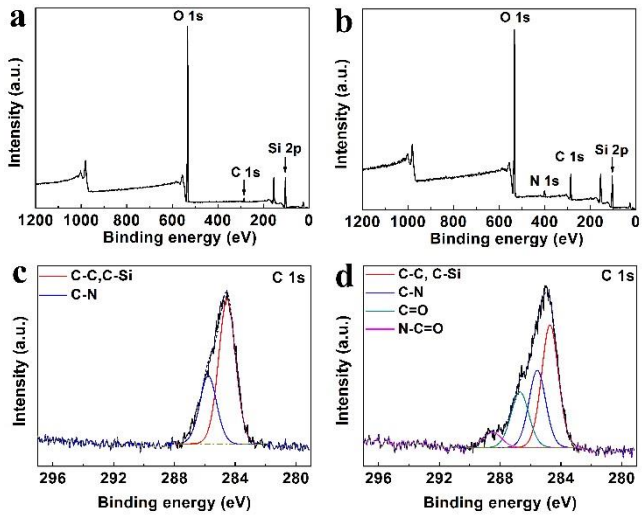

Fig. 2 XPS survey scan of a) SBA-15 and b) SBA-15-CH3-NH2; the corresponding fine spectra of c) SBA-15-CH3-NH2 and d) SBA-15-CH3-IBA.

The initial results indicate that SBA-15-CH_3-IBA with both aptamer and hydrophobicity modification is the best material for insulin enrichment. The design SBA-15-CH_3-IBA (Fig. S5b) has better performance comparing to SBA-15-IBA (Fig. S5c) which suggests that the hydrophobicity plays an important role in the insulin enrichment. The conclusion is consistent with previous reports.[13, 37] The modifications of IBA and -CH_3 into mesopores enhanced the enrichment efficiency (0.05 ng ml^{-1}) since the outer modified group has a worse detection limit (0.5 ng ml^{-1}). The reason is more IBA and CH_3 can be modified into nanoparticle when the inner surface is accessible. The detection limit of 0.05 ng ml^{-1} in serum is much lower than in most of the non-antibody based (116-290 ng ml^{-1})[38-40] or aptamer based (20-58 ng ml^{-1})[20, 22] enrichments, and comparable to antibody based detection.[30]

After confirming the designed SBA-15-CH_3-IBA is the optimal material for insulin enrichment, a further application using enrichment to enhance ELISA was conducted. Fig. 3a shows the standard curve of a commercial ELISA kit, which is obtained by testing the standards in this kit following the instruction provided by manufacturer (Scheme S1). All the standards in this kit are in human serum, and the quantification limit is 7.7 pg ml^{-1}. To achieve a better detection efficiency and conduct the quantification analysis in lower concentration, the designed SBA-15-CH_3-IBA was applied to pre-treat samples. A series of diluted insulin standard solutions with ultra-low concentration (0.25-5 pg ml^{-1}) were tested by ELISA after pre-treatment. The quantification in low concentration range (0.25-5 pg ml^{-1}) is achieved as shown in the standard curve (Fig. 3b) of enhanced ELISA. The linear regression coefficient (R^2) is 0.9556, which is not perfect linear but sufficient for quantification in low concentration range (pg ml^{-1}). The results indicate that with the help of designed SBA-15-CH_3-IBA, the detection sensitivity of commercial ELISA kit increased. The limit-of-detection (0.25 pg ml^{-1}) is 30 times better than that of commercial ELISA kit (7.7 pg ml^{-1}).

To further confirm the quantification ability, a standard addition technique was employed and a recovery rate was calculated (see SI).[35] In our case, a recovery rate of 71% was achieved, which is comparable to the recovery rates in previous studies generally conducted at high concentrations.[37, 38] For example, a study used self-assembled TiO_2 nanocrystal clusters to enrich beta-casein (0.75mg ml^{-1}) and achieved a recovery efficiency of 50%.[36] In another study, the recovery rate of glycopeptide (1μg $μl^{-1}$) enriched by functionalized magnetic nanoparticles is 77.8%.[37] By comparing with literatures, a recovery rate of 71% in the very low concentration of 0.25-5 pg ml^{-1} is significant.

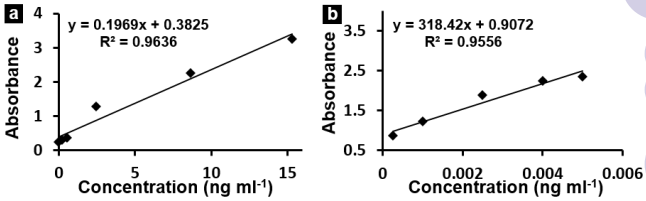

Fig. 3 Standard curves showing the quantification range of (a) commercial ELISA kit, (b) ultrasensitive ELISA with pre-treatment by combo-pore-CH_3-IBA.

In conclusion, we have successfully synthesized mesoporous nanomaterials with co-modified aptamer and methyl groups. When applying this material in the combo-pore approach[7] for pre-treatment of low-abundant bio-samples before ELISA, more sensitive and quantitative detection of insulin in serum can be achieved comparing to commercial ELISA kit. This exploratory study suggests a great potential for enhancing the efficiency of current detection strategies by rationally designed nanomaterials.

The authors acknowledge the financial support from the Australian Research Council, the Queensland Government, the Australian National Fabrication Facility, the Australian Microscopy and Microanalysis Research Facility at the Centre for Microscopy and Microanalysis, the CAS/SAFEA International Partnership Program for Creative Research Teams, The University of Queensland.

Notes and references

1 S. Craft, E. Peskind, M. W. Schwartz, G. C. Schellenberg, M. Raskind and D. Porte, Neurology, 1998, 51, 926-926.
2 P. H. Sonksen, J Endocrinol, 2001, 170, 13-25.
3 F. J. Gil-Bea, M. Solas, A. Solomon, C. Mugueta, B. Winblad, M. Kivipelto, M. J. Ramirez and A. Cedazo-Minguez, J Alzheimers Dis, 2010, 22, 405-413.
4 J. Villanueva, J. Philip, D. Entenberg, C. A. Chaparro, M. K. Tanwar, E. C. Holland and P. Tempst, Anal Chem, 2004, 76, 1560-1570.
5 M. Thevis, A. Thomas, P. Delahaut, A. Bosseloir and W. Schanzer, Anal Chem, 2005, 77, 3579-3585.
6 M. P. Tiwari and B. B. Prasad, J Chromatogr A, 2014, 1337, 22-31.
7 M. M. Moein, M. Javanbakht and B. Akbari-adergani, Talanta, 2014, 121, 30-36.
8 L. Dou and I. S. Krull, Anal Chem, 1990, 62, 2599-2606.
9 S. Ravi, K. K. Peh, Y. Darwis, B. K. Murthy and T. R. R. Singh, Chromatographia, 2007, 66, 805-809.
10 G. Khaksa, K. Nalini, M. Bhat and N. Udupa, Anal Biochem, 1998, 260, 92-95.
11 J. Groen, C. E. Kamminga, A. F. Willebrands and J. R. Blickman, J Clin Invest, 1952, 31, 97-106.
12 N. T. Ditto, T. R. Kline, P. D. Alfinito and J. R. Slemmon, 2009, 182, 260-265.
13 C. Lei, O. Noonan, S. Jambhrunkar, K. Qian, C. Xu, J. Zhang, A. Nouwens and C. Z. Yu, Small, 2014, 10, 2413-2418.
14 C. K. Chiang, W. T. Chen and H. T. Chang, Chem Soc Rev, 2011, 40, 1269-1281.
15 R. J. Tian, H. Zhang, M. L. Ye, X. G. Jiang, L. H. Hu, X. Li, X. H. Bao and H. F. Zou, Angew Chem Int Edit, 2007, 46, 962-965.
16 M. T. Hurley, Z. F. Wang, A. Mahle, D. Rabin, Q. Liu, D. S. English, M. R. Zachariah, D. Stein and P. DeShong, Adv Funct Mater, 2013, 23, 3335-3343.
17 S. D. Jayasena, Clin Chem, 1999, 45, 1628-1650.
18 M. Holmberg and X. L. Hou, Langmuir, 2009, 25, 2081-2089.
19 H. N. Wang, X. F. Zhou, M. H. Yu, Y. H. Wang, L. Han, J. Zhang, P. Yuan, G. Auchterlonie, J. Zou and C. Z. Yu, J Am Chem Soc, 2006, 128, 15992-15993.
20 T. G. Cha, B. A. Baker, M. D. Sauffer, J. Salgado, D. Jaroch, J. L. Rickus, D. M. Porterfield and J. H. Choi, Acs Nano, 2011, 5, 4236-4244.
21 J. F. Xiao, J. A. Carter, K. A. Frederick and L. B. McGown, J Sep Sci, 2009, 32, 1654-1664.
22 X. Y. Zhang, S. C. Zhu, C. H. Deng and X. M. Zhang, Chem Commun, 2012, 48, 2689-2691.
23 X. Wang, Y. Liu, S. J. Wang, D. H. Shi, X. G. Zhou, C. Y. Wang, J. Wu, Z. Y. Zeng, Y. J. Li, J. Sun, J. D. Wang, L. J. Zhang, Z. G. Teng and G. M. Lu, Appl Surf Sci, 2015, 332, 308-317.
24 H. Salmio and D. Bruhwiler, J Phys Chem C, 2007, 111, 923-929.
25 S. M. Darby, M. L. Miller, R. O. Allen and M. LeBeau, J Anal Toxicol, 2001, 25, 8-14.
26 W. Kern, C. Benedict, B. Schultes, F. Plohr, A. Moser, J. Born, H. L. Fehm and M. Hallschmid, Diabetologia, 2006, 49, 2790-2792.
27 T. Kuuranne, A. Thomas, A. Leinonen, P. Delahaut, A. Bosseloir, W. Schanzer and M. Thevis, Rapid Commun. Mass Spectrom., 2008, 22, 355-362.
28 A. Thomas, W. Schanzer, P. Delahaut and M. Thevis, Drug Test Anal, 2009, 1, 219-227.
29 S. Pichini, R. Ventura, I. Palmi, S. di Carlo, A. Bacosi, K. Langohr, R. Abellan, J. A. Pascual, R. Pacifici, J. Segura and P. Zuccaro, J Pharmaceut Biomed, 2010, 53, 1003-1010.
30 E. N. M. Ho, T. S. M. Wan, A. S. Y. Wong, K. K. H. Lam and B. D. Stewart, J Chromatogr A, 2011, 1218, 1139-1146.
31 D. H. Pan, P. Yuan, L. Z. Zhao, N. A. Liu, L. Zhou, G. F. Wei, J. Zhang, Y. C. Ling, Y. Fan, B. Y. Wei, H. Y. Liu, C. Z. Yu and X. J. Bao, Chem Mater, 2009, 21, 5413-5425.
32 S. Jarnbhrunkar, M. H. Yu, J. Yang, J. Zhang, A. Shrotri, L. Endo-Munoz, J. Moreau, G. Q. Lu and C. Z. Yu, J Am Chem Soc, 2013, 135, 8444-8447.
33 M. Kruk, M. Jaroniec, C. H. Ko and R. Ryoo, Chem Mater, 2000, 12, 1961-1968.
34 X. S. Zhao and G. Q. Lu, J Phys Chem B, 1998, 102, 1556-1561.
35 M. C. Estevez, Y. F. Huang, H. Z. Kang, M. B. O'Donoghue, S. Bamrungsap, J. L. Yan, X. L. Chen and W. H. Tan, Methods Mol Biol, 2010, 624, 235-248.
36 J. El-Gindi, K. Benson, L. De Cola, H. J. Galla and N. S. Kehr, Angew Chem Int Edit, 2012, 51, 3716-3720.
37 J. Buijs, C. C. Vera, E. Ayala, E. Steensma, P. Hakansson and S. Oscarsson, Anal Chem, 1999, 71, 3219-3225.
38 A. R. Bhat and H. F. Wu, Rapid Commun. Mass Spectrom., 2010, 24, 3547-3552.
39 A. Greiderer, M. Rainer, M. Najam-ul-Haq, R. M. Vallant, C. W. Huck and G. K. Bonn, Amino Acids, 2009, 37, 341-348.
40 M. Thevis, A. Thomas, P. Delahaut, A. Bosseloir and W. Schanzer, *Anal Chem*, 2006, **78**, 1897-1903.